M.A.L. Nicolelis (Ed.)
Progress in Brain Research, Vol. 130

CHAPTER 6

Temporal and spatial coding in the rat vibrissal system

Ehud Ahissar [1,*] and Miriam Zacksenhouse [2]

[1] *Department of Neurobiology, The Weizmann Institute of Science, Rehovot 76100, Israel*
[2] *Faculty of Mechanical Engineering, Technion – Israel Institute of Technology, Haifa 32000, Israel*

Peripheral encoding

In light of the spatio-temporal nature of the world around us, it is not surprising that sensory encoding is based on spatial and temporal cues that encode static and dynamic events. Spatial encoding of the world is accomplished by arrays of receptors, which are spatially organized across the sensory organs. Each receptor is most sensitive to a specific and limited range within the sensation spectrum. For example, each hair cell in the cochlea is most sensitive to a limited range of acoustic frequencies, which is mapped to a specific location along the cochlea. Each photoreceptor in the retina is sensitive to a limited range of the visual field, and the receptive field (RF) of each mechanoreceptor on the skin is restricted to a limited area of the skin.

Temporal encoding is attained by the temporal pattern of receptor firing. Interestingly, temporal encoding is not limited to the dynamic aspects of the stimulus, and can also be used for encoding stationary aspects. For the latter, the stationary stimulus is modulated by the sensing organ, as, for example, in active touch. Primates explore the texture of objects by moving their fingers across it, and rodents scan their environment by moving their whiskers. Changes in pressure, caused by the presence of an object, or by the ridges and grooves across its surface, are detected by the mechanoreceptors. The temporal intervals between such changes, detected by the same or different receptors, represent spatial distances ($dx = v(t)dt$; where dx is a spatial interval, $v(t)$ is the scanning velocity and dt is a temporal interval). Similarly, fixational eye movements might be used to scan objects visually, with changes in illumination across the surface being detected by the photoreceptors. As in the tactile case, the temporal intervals between such changes represent spatial distances (Ahissar and Arieli, 1997).

Most receptors respond mainly (or only) to *changes* in the sensed signal. Thus, the endogenous movements of the sensory organs may have evolved to provide sufficient changes in the sensed stimulus, even when the environment is stationary. Active sensing is significantly more advantageous than passive sensing, which relies heavily on external changes. Furthermore, active sensing facilitates 'hyper-acuity', that is, higher resolution than that allowed by receptor size or spacing. Hyper-acuity is enabled by the scanning movements, which cover the space within the receptive field of a single receptor, and between adjacent receptors. The encoding here is temporal: relative distances are represented by temporal intervals between the respective responses.

Vibrissal encoding of object location

The rat vibrissal system provides a clear example of dissociated coding schemes. The mystacial pad contains about 35 large whiskers, which are arranged in 5 rows and about 7 arcs (columns) with different lengths (Fig. 1). During whisking, the whiskers move back and forth with a rhythmic motion at 4–10 Hz (Welker, 1964; Carvell and Simons, 1990; Fanselow

---

[*] Corresponding author: Ehud Ahissar, Department of Neurobiology, The Weizmann Institute of Science, Rehovot 76100, Israel. Tel.: +972-8-934-3748; Fax: +972-8-934-4140; E-mail: ehud.ahissar@weizmann.ac.il

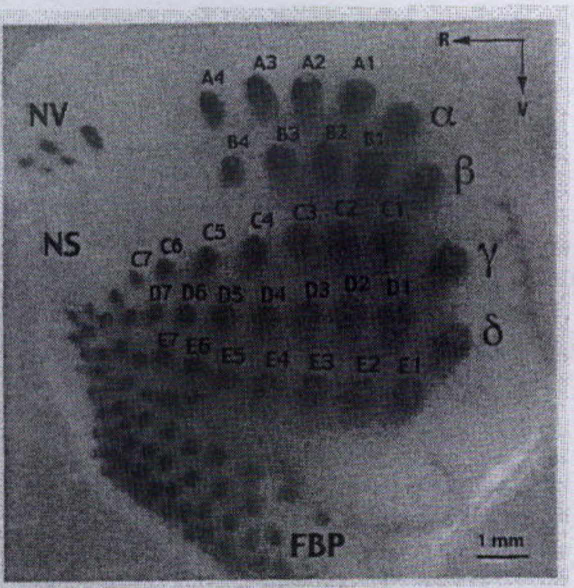

Fig. 1. Spatial organization of the mystacial vibrissae of the rat. Blood sinuses surrounding whiskers' roots were visualized using xylene (see Haidarliu and Ahissar, 1997). A–E, rows; 1–7, arcs; α–δ, straddlers; NV, nasal vibrissae; NS, nostril; FBP, furry buccal pad. Courtesy of S. Haidarliu.

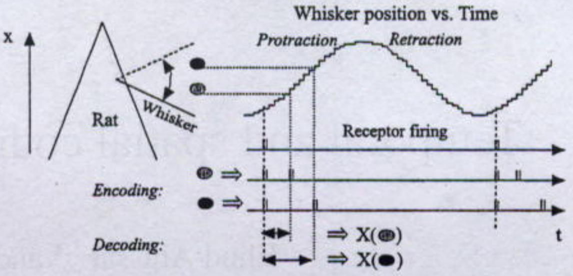

Fig. 2. Temporal encoding during whisking. Only a single whisker and representative brief bursts are depicted for simplicity. Bursts of spikes are generated by the whisker's receptors at the beginning of each protraction cycle, due to velocity threshold crossing (Zucker and Welker, 1969; Brown and Waite, 1974; Shipley, 1974; Nicolelis et al., 1995). The length of this burst probably depends on the profile of whisker movement. Another burst is generated by the same or other receptors at the whisker's root, when the whisker hits an external object (Zucker and Welker, 1969; Brown and Waite, 1974). The temporal interval between the onsets of the two bursts encodes the spatial interval between protraction onset and object location. A more forward location (black ellipsoid) will produce a longer interval. These temporal intervals have to be decoded to represent horizontal object location.

and Nicolelis, 1999; Kleinfeld et al., 1999), thus covering several cubic centimeters near the snout (Wineski, 1983; Brecht et al., 1997). Each whisker along the same arc scans a different trajectory while all the whiskers of the same row scan roughly the same trajectory (Brecht et al., 1997). Thus, spatial information along the vertical axis can be obtained by comparing the activity of individual whiskers along the same arc. The extraction of spatial information about the location of the object in the horizontal plane is more complicated.

Whisking facilitates continuous scanning of the environment along each row of whiskers (Brecht et al., 1997). The horizontal location of an object is encoded by the temporal interval between whisker firing at protraction onset and whisker firing when it hits the object (Fig. 2). Thus, although whisking facilitates hyper-acuity, it has a price. Encoding takes time, and furthermore, the simple coding provided by labeled lines, that is, 'tell me *which* whisker fires[1] and I'll tell you the location of the object', is not sufficient. The brain has to know *when* the whisker fired in order to decode the location of the object. Thus, determination of the horizontal location (relative to whisker position at protraction onset) requires temporal processing of the pattern of activity of the whiskers.

Similar temporal information is contained in the firing patterns of all whiskers that touch an object during whisking. In fact, horizontal object location can be extracted by processing the pattern of activity of individual whiskers. Further information can be obtained later by lateral comparisons along the row. For example, the radial distance of an object from the snout might be computed by triangulation involving the angles that the different whiskers along the row make when hitting the object. Alternatively, decoding might be inherently spatio-temporal, and take into consideration the activity of all the whiskers along the same row simultaneously. In the latter case, both signal to noise ratio and decoding efficiency would probably be improved. In this review we do not attempt to distinguish between these two alternatives, assuming that both should obey similar principles of temporal decoding.

---

[1] The term 'whisker firing' is used here to denote firing of whisker's receptors.

Parallel afferent pathways

Vibrissal information is conveyed to the somatosensory ('barrel') cortex via two parallel pathways, the lemniscal and paralemniscal (Bishop, 1959; Diamond and Armstrong-James, 1992; Woolsey, 1997). The lemniscal pathway, which ascends via the ventral posterior medial nucleus (VPM) of the thalamus, contains large-diameter axons (Bishop, 1959) that end in focal, clustered terminals (Williams et al., 1994). Lemniscal neurons respond at short latency and have relatively small RF centers (Diamond, 1995). The paralemniscal pathway, which ascends via the medial division of the posterior nucleus (POm) of the thalamus, contains smaller-diameter axons that form widespread terminal patterns (Williams et al., 1994). Paralemniscal neurons exhibit slower responses and larger RF centers (Diamond, 1995). These two pathways form two distinct thalamocortical loops. The VPM projects to the barrels in layer 4 and to layers 5b and 6a, and receives feedback from layers 5b and 6a (Chmielowska et al., 1989; Lu and Lin, 1993; Bourassa et al., 1995). The POm projects to layers 1 and 5a and to the inter-barrel septa in layer 4 (Koralek et al., 1988; Lu and Lin, 1993; Diamond, 1995) and receives feedback from layers 5 and 6b (Lu and Lin, 1993; Bourassa et al., 1995).

The existence of two nearly parallel pathways to the cortex has been puzzling. One possibility, which relies on the strong cortico-POm connections (Hoogland et al., 1988; Diamond et al., 1992), suggests that the POm implements an integrative cortico-thalamo-cortical loop, and does not process vibrissal information directly (Hoogland et al., 1988; Diamond, 1995). However, such an interpretation leaves the ascending sensory connections to the POm unexplained. An alternative possibility is that the paralemniscal pathway processes sensory information that is different from the information processed by the lemniscal pathway, and whose processing requires strong cortical feedback and longer delays.

Recently, we provided evidence that is consistent with the latter scheme. In anesthetized rats, we showed that the temporal frequency of whisker movements is represented differently in the two pathways: by response amplitude (and, as a result, spike count) in the lemniscal, and by latency (and, as a result, spike count) in the paralemniscal pathway (Ahissar et al., 1998). These internal representations are first expressed in the thalamus (Sosnik et al., 2001), and are preserved in the corresponding cortical domains (Ahissar et al., 2001). Representation-wise, the thalamo-cortical coupling is more significant in this system than the columnar affiliation in the cortex. This was evident during vertical penetrations into the cortex. When recording from the lemniscal layers, 4 and 5b, the response latency was usually constant for stimulation frequencies between 2 and 11 Hz. However, when recording from the paralemniscal layer 5a, a robust latency representation of the whisker frequency emerged. Thus, although the two different thalamo-cortical systems share the same cortical 'columns', they utilize different coding schemes to represent the whisker frequency.

So far, these observations have only been obtained in anesthetized animals. However, in anesthetized animals, the physiological conditions of the neurons are affected by the anesthesia, and the motor–sensory loop is 'open', that is, sensory acquisition does not depend on the motor system, as it does during whisking. Recent studies demonstrated that the effect of both these factors on response latency is small, on the order of a few milliseconds (Simons et al., 1992; Fanselow and Nicolelis, 1999; Friedberg et al., 1999). Thus, the effects of anesthesia on latency are much smaller than the tens of milliseconds latency variations observed in the paralemniscal pathway. Consequently, sensory neurons would not be expected to behave qualitatively different just because the animal is awake or whisking. Yet, natural whisking may induce specific computational constraints that are not expressed in the anesthetized animal. Thus, the working hypothesis developed here should ultimately be tested in freely moving animals performing object localization or identification during natural whisking.

Decoding and re-coding by the brain: a working hypothesis

Herein, *decoding* refers to the extraction of information encoded in the transmitted signal, and *re-coding* refers to the representation of the same information using another coding scheme. The brain probably performs both operations simultaneously (Perkel and

Bullock, 1968). Our experimentally driven working hypothesis is that the lemniscal pathway decodes spatially encoded information, whereas the paralemniscal system decodes temporally encoded information. Both types of information are obtained during whisking, and encode spatial parameters, such as the location of objects in the surrounding space.

Temporal decoding

In principle, temporally encoded information can be decoded using either a 'passive' or 'active' strategy (Fig. 3A). Passive decoding employs feedforward arrays of time-sensitive elements, such as delay lines (Jeffress, 1948) or synaptic time constants (Buanomuno and Merzenich, 1995), to convert temporal intervals to either labeled-line or population rate coding. Active decoding utilizes internal oscillations as 'temporal rulers', or temporal expectations, against which the temporal interval between input events is compared. This comparison can be implemented by open or closed loops and can result in a labeled-line or a population rate code (Ahissar, 1995).

Whereas delay lines are inefficient for decoding temporal intervals greater than a few milliseconds (Carr, 1993), oscillation-based circuits are efficient particularly in this range (Ahissar, 1998). This suggests that delay-line solutions should be favored for processing temporal intervals in the microsecond range, which occur in binaural localization or echolocation systems, while oscillatory solutions should be preferable for processing intervals in the millisecond (a few to a few hundreds) range, which occur in visual or tactile perception. In fact, single-cell oscillators exist in the somatosensory and visual cortices. In the barrel cortex, the majority of oscillators have a spontaneous frequency around 10 Hz (Ahissar et al., 1997), which is suitable for decoding (by means of comparison) temporal information obtained during whisking. Interestingly, cortical oscillators in other species and other modalities exhibit frequency ranges that also match their corresponding sensory channels. Somatosensory oscillators in the monkey oscillate mostly around 30 Hz (Ahissar and Vaadia, 1990; Lebedev and Nelson, 1995), which is suitable for temporal information carried by rapidly adapting fibers (Talbot et al., 1968; Johansson et al., 1982). Visual oscillations are mostly in the alpha (around 10 Hz) and gamma (40–100 Hz) ranges (Eckhorn et al., 1993; Gray and McCormick, 1996), matching the alpha and gamma ranges of retinal activation frequencies caused by the miniature eye movements (Bengi and Thomas, 1972; Eizenman et al., 1985) (see Ahissar and Arieli, 1997).

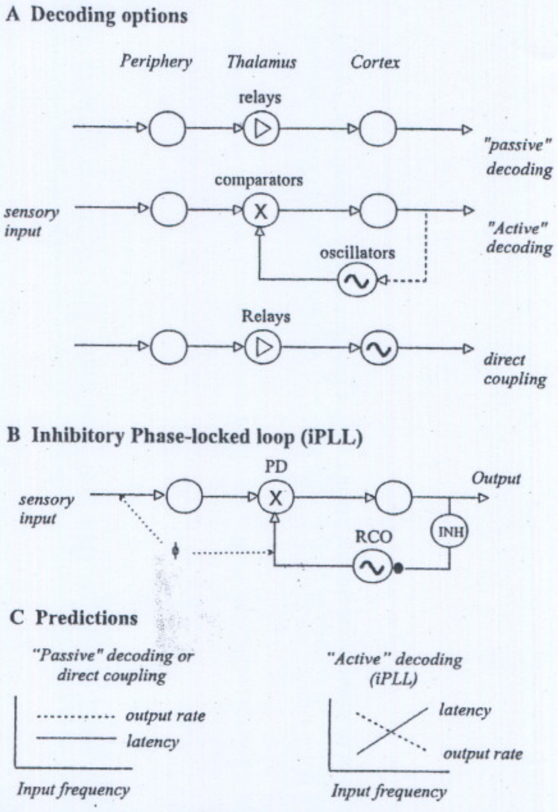

Fig. 3. Possible mechanisms for temporal decoding. (A) Passive decoding is assumed to flow through feedforward connections, where the activity at each level depends on the activity at a lower (more peripheral) level. Arrows represent feedforward elements including 'simple' axons, delay lines, and synapses. Active decoding involves an independent cortical source of information – local oscillators. Information flows both ways and is compared, in this example, in the thalamus. The circuits can be closed (dashed lines) or open loops. In direct coupling, the cortical oscillators are *forced* by the input via relay neurons. (B) The thalamo-cortical inhibitory phase-locked loop (iPLL) decoder. PD, phase detector; RCO, rate-controlled oscillator; INH, inhibitory neurons; •, inhibitory connection; ϕ, phase-difference between the sensory input and the oscillator. (C) Predicted dependencies of thalamic and cortical responses on the input frequency. Adapted from Ahissar et al. (1997).

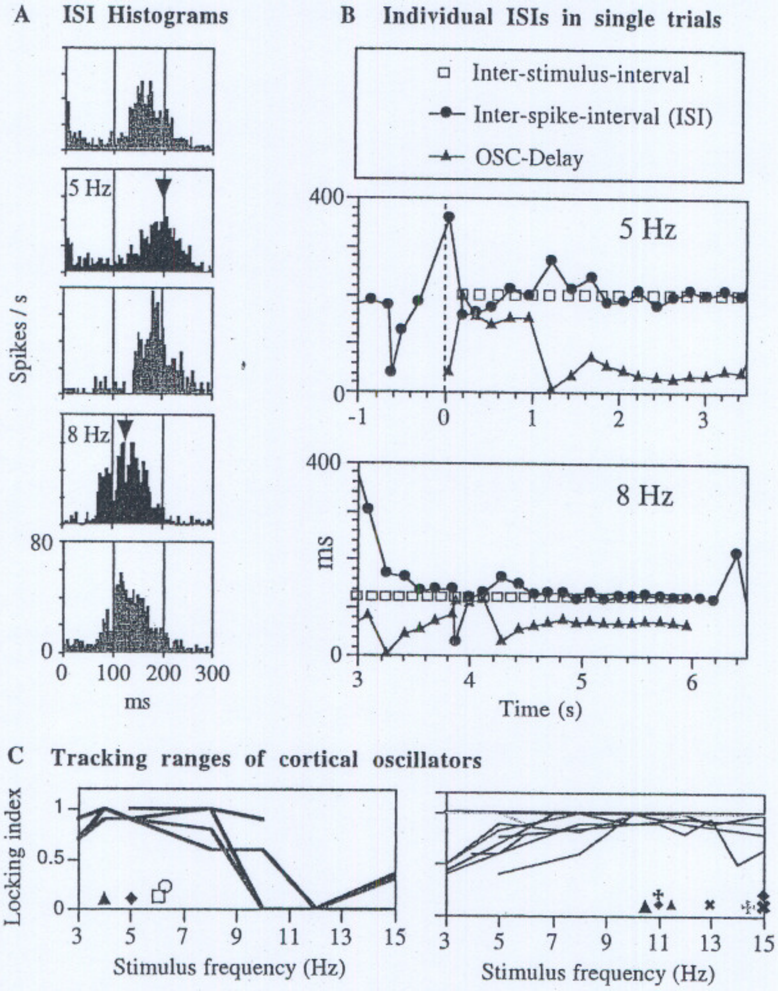

Fig. 4. Frequency locking of single-cell cortical oscillators (OSCs). (A and B) An OSC recorded from layer 2–3 of the barrel cortex of an anesthetized rat during stimulations of whisker E2 with square-wave stimuli. (A) ISI histograms computed for the entire stimulation periods (black) and the interleaved spontaneous periods (gray). Red arrows point to the inter-stimulus intervals. (B) Lock-in dynamics during single stimulus trains. ISIs (black circles), inter-stimulus intervals (open squares), and OSC delays (gray triangles) are plotted as a function of time. Time 0 and the dashed line denotes the beginning of a stimulus train. Note the 1 : 1 firing (one OSC spike per stimulus cycle) and constant phase difference during stabilized states. In the trial presented in the lower panel, the OSC remained 'locked' for 2 additional cycles after the stimulus train ended. The *sensitivity* value extracted from the steady-state data is: $\sigma = d\phi/dI \approx (160 - 55)/(200 - 125) = 1.4$. Note that the phase difference, ϕ, here is the complement of the OSC delay (see text). (C) Frequency locking ranges for 13 single-cell oscillators of the barrel cortex. Symbols show the spontaneous frequencies of these oscillators. Locking index $= 1 - |f_i - f_o|/(f_i + f_o)$ where f_i is the stimulation frequency, and f_o is the oscillator frequency during stimulation. Oscillators were grouped (left and right panels) according to their locking ranges. Adapted from Ahissar et al. (1997).

Oscillation-based temporal decoders could involve open or closed loops (Ahissar, 1995). Of the two, the closed loop is the more efficient, since it is more adaptive, and thus requires fewer elements to achieve a given decoding resolution. Indeed, in the rat vibrissal system, we found evidence for the operation of an oscillation-based closed-loop system. This loop, known as the phase-locked loop (PLL, Ahissar, 1998; see also Kleinfeld et al., 1999), provides specific predictions for neuronal activity during periodic, or frequency modulated (FM), stimuli. One prediction is that the cortical oscillators should follow the external frequency during whisker stimulation. Indeed, within specific frequency ranges, this was the case with most barrel cortex oscillators (Fig. 4; see Ahissar et al., 1997). Another prediction is that the latency and intensity of the responses to periodic stimuli should be inversely related (Fig. 3C). The expected inverse relationship was found in the paralemniscal, but not in the lemniscal, system (Fig. 5; Ahissar et al., 2000). In the paralemniscal system, the latency increases with increasing stimulus frequencies, while the spike count (per stimulus cycle) decreases. This direction of the relationships indicates that the neuronal implementation of the PLL includes inhibition, and is therefore referred to as iPLL (Ahissar, 1998). Since cortico-POm connections probably do not send collaterals to the reticular nucleus of the thalamus (Bourassa et al., 1995), the inhibition in this loop should be cortical.

The main principles of decoding by thalamo-cortical PLL circuits are: (i) the input timing (from the whiskers) is compared at the thalamus against the timing of the cortical oscillations; and (ii) the oscillation frequency is controlled by the resulting 'error signal' so as to match the input frequency (negative feedback). The PLL is an optimal temporal decoder, since it implements a narrow band-pass filter, which adapts its center frequency to match the input frequency (Gardner, 1979). By implementing PLLs, thalamo-cortical loops convert temporally encoded information into a rate-population code. This conversion is monotonic within a limited range of input frequencies, which determines the working range (see Section 'Sensitivity, gain, and working range').

Conversion of temporal code to rate-population code

The main components of the iPLL are (Fig. 3B) the thalamic phase detector (PD), the inhibitory neuron (INH) and the cortical rate-controlled oscillator (RCO). The information in the input to the PLL is encoded temporally in the inter-event intervals. The PLL re-encodes this information in the form of rate code at the output of the PD. This process is accomplished in three stages: (1) phase detection, (2) rate conversion, and (3) adaptation. Phase detection and rate conversion are accomplished by the PD, whose total output decreases with the detected phase difference. This is probably implemented by a simple

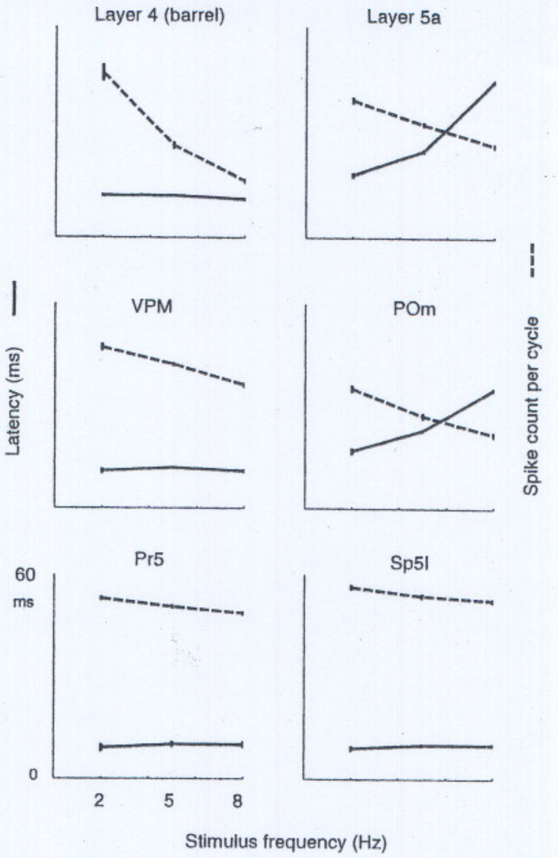

Fig. 5. Typical steady-state tuning curves of local neuronal populations along the two sensory pathways. Examples of pooled single and multi-units recorded from single electrodes in the brainstem (Pr5 and Sp5I nuclei), thalamus (VPM and POm nuclei), and cortex (layer 4, barrels, and layer 5a, non-barrels). Stimuli were air-puffs directed to several whiskers of 1 or 2 rows (3 s trains of 50 ms pulses in the protraction direction for all frequencies; (Ahissar and Haidarliu, 1998). Graphs depict the mean ± S.E.M (small vertical bars), during steady state ($0.5 < t < 3$ s), of response latency (solid lines, latency to half-height rising edge of the PSTH) and response magnitude (broken lines, spike counts per stimulus cycle). Brainstem responses exhibited a negligible, if any, dependency on the stimulus frequency. Lemniscal thalamo-cortical latencies were constant, whereas spike counts decreased with increasing frequencies. Paralemniscal latencies and spike counts exhibited inverse dependencies: latencies increased, whereas spike counts decreased with increasing stimulus frequencies. Latencies are plotted with a common scale (0 to 60 ms), whereas spike counts are plotted with independent arbitrary scales that emphasize the relative values for each local population. Although the absolute spike count values varied significantly between different local populations, their frequency dependency patterns were typical for each nucleus or cortical layer. Latency values were consistent within each nucleus and cortical layer.

AND gating at the thalamus (Ahissar, 1998). The critical variable is the total output of the PD over a single cycle of the RCO, or equivalently the average rate over the relevant unit of time provided by the period of the oscillator. The instantaneous rate of the PD does not matter. For example, one possible implementation (Ahissar et al., 1997) considers a PD whose active instantaneous rate is constant. Varying the active duration inversely with the phase-difference controls the total output of the PD along the cycle.

Adaptation is accomplished by the RCO, whose period is affected by the output rate of the PD. By virtue of the closed loop, the RCO tunes its period to match that of the input. The tuning affects the phase relationship with the input events, and thus, the corresponding output from the PD. Upon reaching a steady state, the PLL uniquely re-encodes the input period in the phase difference and the output rate. Tuning also enables the PLL to quickly detect changes in the period of the input, which has been internally represented as expectations in the form of the adapted period of the RCO. Both of these capabilities may be characterized by the *sensitivity* of the PLL.

Sensitivity, gain, and working range of the PLL

The period of the RCO varies in order to match the period of the input (see previous section). When a periodic input is applied, a stable PLL will reach a new steady state in which the RCO oscillates at the period of the input and maintains a constant phase difference[2] relative to the input events. In such a case, the steady-state phase re-encodes the period of the input, and is further encoded by the steady-state output rate of the PD. This process depends critically on the open-loop gain of the PLL.

The open-loop gain, β, determines the change in the period of the RCO due to a small change in the phase difference, and is given by the product of the PD and RCO gains. (The PD gain determines the change in the output rate of the PD due to a small change in the phase, and the RCO gain determines the change in the period of the RCO due to a small change in its input.) When both the PD and the RCO are linear, the gains of the PD and RCO are constant, and so is the open-loop gain. In other instances, the gains may vary with the frequency. The open-loop gain determines the internal loop dynamics and thus also the stability of the PLL (Ahissar, 1998); it should be less than 2 for the PLL to be stable, and less than 1 for it to be monotonically stable[3]. Note that these are the same stability conditions as for a forced oscillator (Perkel et al., 1964).

A critical aspect of the PLL is that it constitutes a closed loop so that changes in the period of the RCO affect the phase difference and thus the subsequent period of the RCO. The overall response of the closed loop is described by the closed-loop gain, which differs from the open-loop gain. The closed-loop gain can be related to one of the output variables of the loop: the output rate or the phase difference. For comparison with forced oscillators, we relate it here to the phase difference and term the corresponding closed-loop gain *sensitivity*. Specifically, the sensitivity, σ is the ratio between variations in the steady-state phase difference and variations in the normalized input period (normalized with respect to the intrinsic period of the RCO). We define $\sigma = \mathrm{d}\phi/\mathrm{d}I$, where $\mathrm{d}\phi$ is the change in the response lead (the complement of the response latency) and $\mathrm{d}I$ is the change in the input period.

The sensitivity of the PLL is inversely related to the open-loop gain ($\sigma = 1 + 1/\beta$; Zacksenhouse, 2001) so the sensitivity of a stable PLL should be larger than 1.5. The sensitivity is also inversely related to the working range, which is the range of input periods over which the phase difference and output rate vary monotonically. Temporal decoding presents the PLL with the contradictory requirements for high sensitivity and a wide working range. Given this, what is the selection made by the nervous system? Extraction of the relevant values from data collected during our cortical and thalamic recordings (Ahissar et al., 1997, 2000) revealed that the brain does not employ high sensitivities; the sensitivity

---

[2] The phase difference can be defined as either the response latency or its complement, the response lead, normalized with respect to the intrinsic period of the RCO.

[3] Note that the polarity of the gain depends on the definition of the phase difference (phase lag versus phase lead).

values were usually larger than 1, but less than 1.5 (see, for example, Fig. 4).

This range (1–1.5) of experimentally estimated decoding sensitivity is further revealing, since it has different implications depending on the nature of the underlying neural circuit. In this section, the implications of the assumption that the cortical oscillators are embedded in PLLs will be considered. In the following section, the implications of the assumption that the cortical oscillators are directly forced will be considered (and rejected). Assuming that the thalamocortical loops implement iPLLs, the estimated sensitivity of 1–1.5 indicates that these loops operate outside the stable range, or at the most on the verge of stability. This conclusion is supported by the observation that during applications of an external periodic stimulus, cortical and thalamic neurons usually toggle between phase-locked (stable) and unlocked periods (Ahissar et al., 1997; Ahissar et al., 2000). Furthermore, the quasi-steady phase locking sections are preceded by phase oscillations (e.g, Fig. 4). These observations further support the conclusion that the neural circuits operate in a high-gain, low-sensitivity regime.

While the high open-loop gain of a PLL has the disadvantage of de-stabilizing the response, it has the advantage of increasing the working range over which the system is sensitive to temporal variations in the input. Indeed, in the paralemniscal system, the tracking ranges of thalamic and cortical neurons are large in comparison to their intrinsic periods. For example, typical tracking ranges stretch from 3 to at least 7–8 Hz (Ahissar et al., 2000, 2001; Sosnik et al., 2000; see Fig. 4), which corresponds to working ranges of >200 ms. If indeed these neurons participate in iPLLs, the intrinsic frequency of the RCOs should be above 7–8 Hz, and thus, these working ranges are significantly larger than the intrinsic period. This can only be achieved with high open-loop gains and low sensitivities ($\beta > 2, \sigma < 1.5$), and thus, would be outside the stability range of the PLL (Ahissar, 1998; Zacksenhouse, 2001). We may conclude that the neural implementation achieves a large working range at the expense of the stability of individual PLLs. In light of this instability of individual PLLs, reliable temporal-to-rate transformation may require the co-operation of a pool of PLLs (see Section 'Weakly coupled PLLs' below).

PLLs versus forced oscillators

Sensitivity analysis provides a tool for discriminating between oscillators embedded within iPLLs and oscillators that are forced directly by the input (Fig. 3). The sensitivity of a forced oscillator is $\sigma = 1/\beta$ (Zacksenhouse, 2001), so a forced oscillator whose sensitivity is larger than 0.5 is stable, and is monotonically stable if its sensitivity is larger than 1. However, although the sensitivity of neurons in the vibrissal system has been estimated to be larger than 1, their response patterns do not exhibit monotonic stability. For example, the sensitivity of the neuron whose response is depicted in Fig. 4 has been estimated to be around 1.4, but its phase oscillates before reaching a steady state. Thus, the sensitivity analysis enables us to reject, at least in this and other similar cases, the hypothesis that the oscillating units are directly forced by the input.

Weakly coupled PLLs

How do unstable PLLs perform reliably and provide meaningful rate code? One appealing explanation relies on a pool of weakly coupled PLLs. The coupling may be achieved at the level of the RCOs. In response to a given input, the percentage of RCOs that phase lock to the input and oscillate at its frequency increases. The weak coupling between the RCOs may then evoke the 'magnet effect' (von Holst, 1973), and thereby attract the rest of the RCOs to oscillate at the same frequency. Indeed, computer simulations support this scenario (E. Ahissar, unpublished observations). Thus, it might be that the rate-coded output should be read out from an ensemble of parallel PLL circuits in order to obtain reliable representations.

Rate-population code at the output of the PLL

Thalamic implementations of PDs most likely involve local populations of a few tens of 'relay' neurons (Ahissar, 1998), whose total spike count (per cycle) establish the output code of the PLL. The basic output code relies on the summed activity across all PD neurons. However, specific implementations may also involve a population-vector code (in addition to the population-sum code), which is based on

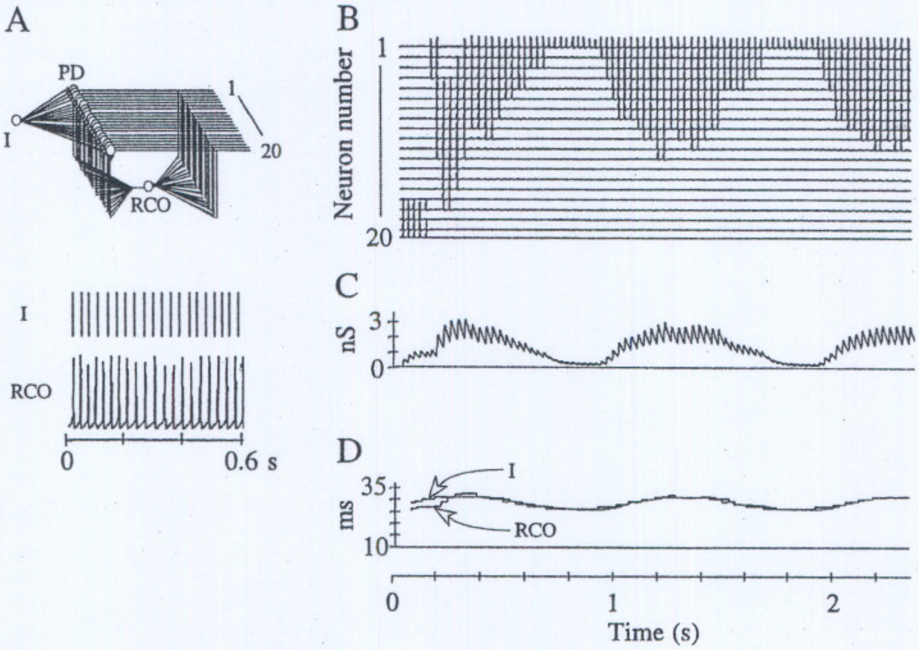

Fig. 6. A computer simulation of the population coding at the output of the PLL. (A) Simulated circuit and spike trains. The circuit was composed of one input cell (I), 20 PD neurons (PD), 20 different delay lines from the input to the PD neurons, and one RCO neuron (RCO) that receives an inhibitory input from each of the 20 PD neurons. The timings of the input spikes and the membrane voltage of the RCO are presented at the bottom. (B) The output of the PLL, which is the population output of the PD. The spike trains of the 20 PD neurons are depicted. Each line represents, as a function of time, the membrane voltage of one PD neuron. (C) The integrated input of the RCO, i.e. the total inhibitory conductance caused by synaptic input to the RCO neuron. (D) The instantaneous ISIs of the input I and the RCO are described as a function of time. After a lock-in stage (whose duration and dynamics depend on the loop gain and the initial phase; Ahissar, 1998), the two curves essentially merge. The simulation was performed on a DEC 3100 workstation using Genesis (Wilson and Bower, 1989) and using Hodgkin–Huxley kinetics. Adapted from Ahissar (1998).

the identity of the active PD neurons, as illustrated in Fig. 6 (see Ahissar, 1998). In this implementation, specific input periods are represented by both (i) specific sets of synchronously active PD neurons and (ii) specific values of the summed activity of all PD neurons. Whether such a population-vector coding takes place is not yet known.

A temporal-to-rate code transformation should result in a cortical rate-coded representation of horizontal object location. PLL simulations demonstrate that when a new object appears within the whisking trajectory, this appearance should evoke a transient response in the PD spike count. The magnitude of the transient response should be proportional to the spatial angle between the position of the protraction onset and the location of the object (Fig. 7), and should depend on the loop sensitivity. This prediction of the PLL mechanism has not yet been tested.

Spatial decoding

Spatial decoding mechanisms commonly involve spatial derivatives (or comparisons) which are obtained by lateral inhibition. In the lemniscal system, spatial decoding may be implemented at the VPM, where lateral inhibition is accomplished via the thalamic reticular nucleus (TRN). The known anatomy and physiology of these two thalamic nuclei (Salt, 1989; Lee et al., 1994) support such a function. However, the massive, well-organized, cortical feedback to the thalamus indicates that this is not the entire story.

Cortical projections to the VPM diverge along the arcs, whereas projections to the TRN (as well as those to the POm) diverge along the rows (Welker et al., 1988). We postulate that this anatomical polarization enables the thalamocortical machinery to focus

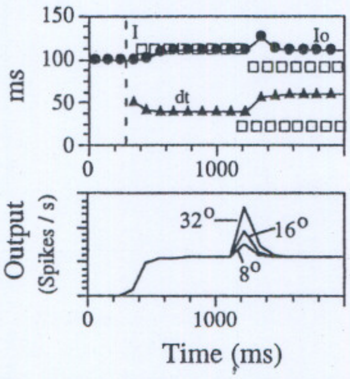

Fig. 7. Computer simulation of an iPLL: Cortical representation of object location. Cortical spontaneous oscillations were at 10 Hz (Io, circles). The whisking (I = 110 ms; squares) commenced at t = 300 ms, and the object was introduced at t = 1200 ms and a spatial angle of 32°. The introduction of the object was simulated by inserting, in every whisking cycle, an additional input spike at the time (20 ms from the protraction onset) when the whisker would have touched the object. After a transient response, the iPLL re-locked to the full whisking cycle, but with a new phase (upper panel; dt is the delay between protraction onset and RCO firing, triangles). Different object locations (8°, 16° and 32°) are represented by different magnitudes of the transient response (lower panel; arbitrary vertical scale). Adapted from Ahissar et al. (1997).

on one specific arc (see Ghazanfar and Nicolelis, 1997), the arc whose whiskers are the first to hit the object. Since the whiskers are not all of the same length (Brecht et al., 1997), the first arc to be activated depends on the radial distance of the object from the animal's snout. The VPM representation of that arc (Haidarliu and Ahissar, 2001) will be depolarized via the arc-oriented cortical feedback, while the VPM representations of the other arcs will be inhibited, via the row-oriented TRN activation. Depolarization moves the VPM cells into a gating mode, which facilitates fine computation (Sherman and Guillery, 1996). Computation might be based on simple lateral comparisons or, more likely, on a closed-loop thalamo-cortical process. In the latter case, the computation may involve cortical expectations and error signals, as in the PLL-based temporal processing carried by the paralemniscal system.

Two types of distinct computational tasks are relevant here: localization and identification. Localization relies on the identity of the activated whisker, and thus, may be determined using lateral comparisons along the arc. Identification relies on the fine textural details of the surface, which are encoded both temporally and spatially. Temporal phase relationships across arc-wise neighboring whiskers represent vertical details, such as offsets or curvatures, while temporal intervals in the activity of individual whiskers represent horizontal details, such as spatial frequency or roughness. The relevant temporal frequencies involved in identification depend on the object's spatial frequencies (Carvell and Simons, 1990) and are usually much higher than those involved in the horizontal localization, which is postulated to be computed by the paralemniscal system. However, the lemniscal system might still utilize the PLL strategy to decode such high-frequency information. If so, the lemniscal system should rely on the higher-frequency cortical oscillations (Ahissar et al., 1997; Jones and Barth, 1999), and should exhibit latency coding of the input temporal frequency in the range of the decoded frequencies (>10 Hz).

Integration

Tactile acquisition by the whiskers is a motor–sensory active process. Whiskers are moved by the motor system to acquire information, which is then analyzed by the sensory system. This system operates in a closed loop, since sensory information drives motor circuits at multiple levels (Kleinfeld et al., 1999). As with any other closed loop, there is no starting point, the process is not more sensory–motor than it is motor–sensory.

The sensory part of the loop contains two parallel pathways: the lemniscal and paralemniscal systems. Our working hypothesis is that the paralemniscal system decodes the low-frequency (whisking-range) temporally encoded information, and that the lemniscal system decodes spatially encoded information and high-frequency (texture-dependent) temporally encoded information. Since temporal decoding by PLLs results in a rate-population code, the integration of all the decoded outputs should be straightforward. Indeed, signs of such integration were observed in layer 2/3 of the barrel cortex (Ahissar et al., 2001). Yet, some anatomical segregation is preserved between these two systems, even at the cortical level (Kim and Ebner, 1999), which suggests that even the sensory–motor control systems operate in parallel, at least up to a later motor stage.

From a functional point of view, the vibrissal system includes three parallel sensory–motor processes. These processes can be distinguished by their decoding of sensory cues; one decodes temporally encoded low-frequency horizontal localization cues, another temporally encoded high-frequency textural cues, and the third, spatially encoded vertical cues. The sensory part of the first process is accomplished by the paralemniscal system, whereas those of the other two are implemented by the lemniscal system. Theoretically, each process could be implemented by a separate sensory–motor loop, and could even have a separate muscular system on the mystacial pad. Alternatively, the three processes could share at least some of the motor circuits and muscles. Although the latter scheme seems more plausible, the stage at which the different processes merge is not yet clear. As with the local sensory loops, the operation of each sensory–motor loop is characterized by its loop gain and sensitivity. The gains of the different sensory–motor loops are probably under global control so that the brain can regulate the strength of the sensory–motor coupling of each loop. This regulation can bring a specific sensory–motor process to the 'foreground', while keeping the other two processes in the 'background', during the performance of a specific task.

Abbreviations

PLL	phase-locked loop
iPLL	inhibitory PLL
ePLL	excitatory PLL
FM	frequency modulation
RCO	rate-controlled oscillator
PD	phase detector
VPM	ventral posterior medial nucleus of the thalamus
POm	medial division of the posterior nucleus of the thalamus
TRN	thalamic reticular nucleus

Non-keyboard characters

sensitivity	σ (Greek sigma)
gain	β (Greek beta)
phase	ϕ (Greek phi)
straddlers	α, β, γ, δ (Greek alpha, beta, gamma, delta)

Acknowledgements

We wish to thank S. Haidarliu and R. Sosnik for their help with the experiments and data analysis and B. Schick for reviewing the manuscript. This work was supported by the United States–Israel Binational Science Foundation (Israel) Grant 97-222 and the MINERVA Foundation, Germany.

References

Ahissar, E. (1995) *Conversion from temporal-coding to rate-coding by neuronal phase-locked loops*. The Weizmann Institute of Science, Rehovot, Technical Report GC-EA/95-4.

Ahissar, E. (1998) Temporal-code to rate-code conversion by neuronal phase-locked loops. *Neural Comput.*, 10(3): 597–650.

Ahissar, E. and Arieli, A. (1997) Seeing through miniature eye movements: A hypothesis. *Neurosci. Lett. Suppl.*, 48: S2.

Ahissar, E. and Vaadia, E. (1990) Oscillatory activity of single units in a somatosensory cortex of an awake monkey and their possible role in texture analysis. *Proc. Natl. Acad. Sci. USA*, 87: 8935–8939.

Ahissar, E., Haidarliu, S. and Zacksenhouse, M. (1997) Decoding temporally encoded sensory input by cortical oscillations and thalamic phase comparators. *Proc. Natl. Acad. Sci. USA*, 94: 11633–11638.

Ahissar, E., Sosnik, R. and Haidarliu, S. (2000) Transformation from temporal to rate coding in a somatosensory thalamocortical pathway. *Nature*, 406: 302–306.

Ahissar, E., Sosnik, R. and Haidarliu, S. (2000) Temporal frequency of whisker movement: II. Laminar organization of cortical representations. *J. Neurophysiol.*, in press.

Bengi, H. and Thomas, J.G. (1972) Studies on human ocular tremor. In: R.M. Kenedi (Ed.), *Prospectives in Biomedical Engineering*. Macmillen, London, pp. 281–292.

Bishop, G.H. (1959) The relation between nerve fiber size and sensory modality: Phylogenetic implications of the afferent innervation of cortex. *J. Nerv. Ment. Dis.*, 128: 89–114.

Bourassa, J., Pinault, D. and Deschenes, M. (1995) Corticothalamic projections from the cortical barrel field to the somatosensory thalamus in rats: a single-fibre study using biocytin as an anterograde tracer. *Eur. J. Neurosci.*, 7: 19–30.

Brecht, M., Preilowski, B. and Merzenich, M.M. (1997) Functional architecture of the mystacial vibrissae. *Behav. Brain Res.*, 84: 81–97.

Brown, A.W. and Waite, P.M. (1974) Responses in the rat thalamus to whisker movements produced by motor nerve stimulation. *J. Physiol.*, 238: 387–401.

Buanomuno, D. and Merzenich, M.M. (1995) Temporal information transformation into a spatial code by a neural network with realistic properties. *Science*, 267: 1028–1030.

Carr, C.E. (1993) Processing of temporal information in the brain. *Annu. Rev. Neurosci.*, 16: 223–243.

Carvell, G.E. and Simons, D.J. (1990) Biometric analyses of vibrissal tactile discrimination in the rat. *J. Neurosci.*, 10: 2638–2648.

Chmielowska, J., Carvell, G.E. and Simons, D.J. (1989) Spatial organization of thalamocortical and corticothalamic projection systems in the rat SmI barrel cortex. *J. Comp. Neurol.*, 285: 325–338.

Diamond, M.E. (1995) Somatosensory thalamus of the rat. In: E.G. Jones and I.T. Diamond (Eds.), *Cerebral Cortex, Vol. 11*. Plenum Press, New York, pp. 189–219.

Diamond, M.E. and Armstrong-James, M. (1992) Role of parallel sensory pathways and cortical columns in learning. *Concepts Neurosci.*, 3: 55–78.

Diamond, M.E., Armstrong-James, M., Budway, M.J. and Ebner, F.F. (1992) Somatic sensory responses in the rostral sector of the posterior group (Pom) and in the ventral posterior medial nucleus (Vpm) of the rat thalamus: dependence on the barrel field cortex. *J. Comp. Neurol.*, 319: 66–84.

Eckhorn, R., Frien, A., Bauer, R., Woelbern, T. and Kehr, H. (1993) High frequency (60–90 Hz) oscillations in primary visual cortex of awake monkey. *NeuroReport*, 4: 243–246.

Eizenman, M., Hallett, P.E. and Frecker, R.C. (1985) Power spectra for ocular drift and tremor. *Vis. Res.*, 25: 1635–1640.

Fanselow, E.E. and Nicolelis, M.A.L. (1999) Behavioral modulation of tactile responses in the rat somatosensory system. *J. Neurosci.*, 19: 7603–7616.

Friedberg, M.H., Lee, S.M. and Ebner, F.F. (1999) Modulation of receptive field properties of thalamic somatosensory neurons by the depth of anesthesia. *J. Neurophysiol.*, 81: 2243–2252.

Gardner, F.M. (1979) *Phaselock Techniques*. Wiley, New York.

Ghazanfar, A.A. and Nicolelis, M.A. (1997) Nonlinear processing of tactile information in the thalamocortical loop. *J. Neurophysiol.*, 78: 506–510.

Gray, C.M. and McCormick, D.A. (1996) Chattering cells: superficial pyramidal neurons contributing to the generation of synchronous oscillations in the visual cortex. *Science*, 274: 109–113.

Haidarliu, S. and Ahissar, E. (1997) Spatial organization of facial vibrissae and cortical barrels in the guinea pig and golden hamster. *J. Comp. Neurol.*, 385: 515–527.

Haidarliu, S. and Ahissar, E. (2001) Size gradients of barreloids in the rat thalamus. *J. Comp. Neurol.*, 429: 372–387.

Von Holst, E. (1973) Relative coordination as a phenomenon and as a method of analysis of central nervous functions. In: R.D. Martin (Ed.), *The Behavioral Physiology of Analysis of Central Nervous Functions of Animals and Man. Selected Papers of Eric von Holst*. University of Miami Press, Coral Gables.

Hoogland, P.V., Welker, E., Van der Loos, H. and Wouterlood, F.G. (1988) The organization and structure of the thalamic afferents from the barrel cortex in the mouse; a PHA-L study. In: M. Bentivoglio and R. Spreafico (Eds.), *Cellular Thalamic Mechanisms*. Elsevier, Amsterdam, pp. 152–162.

Jeffress, L.A. (1948) A place theory of sound localization. *J. Comp. Physiol. Psychol.*, 41: 35–39.

Johansson, R.S., Landstrom, U. and Lundstrom, R. (1982) Responses of mechanoreceptive afferent units in the glabrous skin of the human hand to sinusoidal skin displacements. *Brain Res.*, 244: 17–25.

Jones, M.S. and Barth, D.S. (1999) Spatiotemporal organization of fast (>200 Hz) electrical oscillations in rat vibrissa/barrel cortex. *J. Neurophysiol.*, in press.

Kim, U. and Ebner, F.F. (1999) Barrels and septa: separate circuits in rat barrels field cortex. *J. Comp. Neurol.*, 408: 489–505.

Kleinfeld, D., Berg, R.W. and O'Connor, S.M. (1999) Anatomical loops and their electrical dynamics in relation to whisking by rat [In Process Citation]. *Somatosens. Mot. Res.*, 16: 69–88.

Koralek, K.A., Jensen, K.F. and Killackey, H.P. (1988) Evidence for two complementary patterns of thalamic input to the rat somatosensory cortex. *Brain Res.*, 463: 346–351.

Lebedev, M.A. and Nelson, R.J. (1995) Rhythmically firing (20–50 Hz) neurons in monkey primary somatosensory cortex: Activity patterns during initiation of vibratory-cued hand movements. *J. Comput. Neurosci.*, 2: 313–334.

Lee, S.M., Friedberg, M.H. and Ebner, F.F. (1994) The role of GABA-mediated inhibition in the rat ventral posterior medial thalamus. I. Assessment of receptive field changes following thalamic reticular nucleus lesions. *J. Neurophysiol.*, 71: 1702–1715.

Lu, S.M. and Lin, R.C. (1993) Thalamic afferents of the rat barrel cortex: a light- and electron-microscopic study using *Phaseolus vulgaris* leucoagglutinin as an anterograde tracer. *Somatosens. Mot. Res.*, 10: 1–16.

Nicolelis, M.A.L., Baccala, L.A., Lin, R.C.S. and Chapin, J.K. (1995) Sensorimotor encoding by synchronous neural ensemble activity at multiple levels of the somatosensory system. *Science*, 268: 1353–1358.

Perkel, D.H. and Bullock, T.H. (1968) Neural coding. *Neurosci. Res. Progr. Bull.*, 6: 221–248.

Perkel, D.H., Schulman, J.H., Bullock, T.H., Moore, G.P. and Segundo, J.P. (1964) Pacemaker neurons: effects of regularly spaced synaptic input. *Science*, 145: 61–63.

Salt, T.E. (1989) Gamma-aminobutyric acid and afferent inhibition in the cat and rat ventrobasal thalamus. *Neuroscience*, 28: 17–26.

Sherman, S.M. and Guillery, R.W. (1996) Functional organization of thalamocortical relays. *J. Neurophysiol.*, 76: 1367–1395.

Shipley, M.T. (1974) Response characteristics of single units in the rat's trigeminal nuclei to vibrissa displacements. *J. Neurophysiol.*, 37: 73–90.

Simons, D.J., Carvell, G.E., Hershey, A.E. and Bryant, D.P. (1992) Responses of barrel cortex neurons in awake rats and effects of urethane anesthesia. *Exp. Brain Res.*, 91: 259–272.

Sosnik, R., Haidarliu, S. and Ahissar, E. (2001) Temporal frequency of whisker movement: I. Representations in brainstem and thalamus. *J. Neurophysiol.*, in press.

Talbot, W.H., Darian-Smith, I., Kornhuber, H.H. and Mountcastle, V.B. (1968) The sense of flutter-vibration: comparison of the human capacity with response patterns of mechanoreceptive afferents from the monkey hand. *J. Neurophysiol.*, 31: 301–334.

Welker, E., Hoogland, P.V. and Van der Loos, H. (1988) Organization of feedback and feedforward projections of the barrel cortex: a PHA-L study in the mouse. *Exp. Brain Res.*, 73: 411–435.

Welker, W.I. (1964) Analysis of sniffing of the albino rat. *Behaviour*, 22: 223–244.

Williams, M.N., Zahm, D.S. and Jacquin, M.F. (1994) Differential foci and synaptic organization of the principal and spinal trigeminal projections to the thalamus in the rat. *Eur. J. Neurosci.*, 6: 429–453.

Wilson, M.A. and Bower, J.M. (1989) The simulation of large-scale neural networks. In: C. Koch and I. Segev (Eds.), *Methods in Neuronal Modeling: from Synapses to Networks.* MIT Press, Cambridge, MA, pp. 291–333.

Wineski, L.E. (1983) Movements of the cranial vibrissae in the golden hamster (*Mesocritus auratus*). *J. Zool. Lond.*, 200: 261–280.

Woolsey, T.A. (1997) Barrels, vibrissae and topographic representations. In: and G. Adelman and B. Smith (Eds.), *Encyclopedia of Neuroscience Vol. I.* Elsevier, Amsterdam, pp. 195–199.

Zacksenhouse, M. (2001) Sensitivity of basic oscillatory mechanisms for pattern generation and decoding. *Biol. Cybern.*, in press.

Zucker, E. and Welker, W.I. (1969) Coding of somatic sensory input by vibrissae neurons in the rat's trigeminal ganglion. *Brain Res.*, 12: 138–156.